Hindawi
Advances in Materials Science and Engineering
Volume 2022, Article ID 1896634, 14 pages
https://doi.org/10.1155/2022/1896634

Research Article

Investigating the Thermo-Physiological Comfort Properties of Weft-Knitted Smart Structures Having a Negative Poisson's Ratio

Muhammad Sohaib Anas,[1] Habib Awais,[1] Syed Talha Ali Hamdani,[1] Khubab Shaker,[2] Zeeshan Azam,[1] and Yasir Nawab[1]

[1]*School of Engineering & Technology, Department of Textile Engineering, National Textile University, Faisalabad 37610, Pakistan*
[2]*School of Engineering & Technology, Department of Materials, National Textile University, Faisalabad 37610, Pakistan*

Correspondence should be addressed to Yasir Nawab; ynawab@ntu.edu.pk

Received 1 September 2022; Revised 10 October 2022; Accepted 27 October 2022; Published 8 November 2022

Academic Editor: Damien Soulat

Smart auxetic structures are gaining attention in various areas such as architecture, clothing (sports and protective), civil, and medical applications owing to their negative Poisson's ratio. Compared to ordinary structures, these structures have better properties (shear resistance, formability, energy absorbance, and robust fracture strength). Auxetic structures show the exceptional property of becoming wider in one direction when stretched from another direction. In this research, three different auxetic weft-knitted structures were fabricated using nylon, polyester, acrylic, and cotton yarns on a Shima Seiki flat-knitting machine. The physical properties, negative Poisson's ratio, and thermo-physiological comfort properties of these fabrics were checked. Negative Poisson's ratio strain curves of the developed fabrics were plotted; all fabrics, except for nylon, show the negative Poisson's ratio (NPR). The NPR decreases with increased strain in the longitudinal direction, and polyester exhibits a maximum value of NPR −0.4 in line structure at 30 mm extension. Results also revealed that structures made with nylon and polyester yarns exhibit a better value of air permeability than acrylic and cotton, while acrylic provides the best thermal resistance values than other materials in line structure and polyester yarn shows better overall moisture management capacity (OMMC) performance in zigzag structures.

1. Introduction

An effect in which the materials or structures extend perpendicular to the directions of applied force is demarcated as Poisson's effect [1, 2]. Typically, Poisson's ratio of isotropic homogeneous structures ranges from −1 to 0.5. Poisson's ratio describes how much structure contracts or expands when we apply force on them. The phenomenon of auxeticity results from the internal structure of the molecules and the way they deform themselves [3]. Due to the axial load, auxetic structures become thicker. On the application of compression load, it becomes thinner because of its hinge-like structure that causes flex when it is stretched. These materials/structures worked well during shear modulus, energy absorption, vibration damping, and sound absorption testing [4]. Auxetic materials have numerous desirable characteristics due to their special quality, including good body fit, better shear resistance, improved indentation resistance, increased plane strain fracture toughness, increased resistance to shock, soundproofing, and other features. There are several possible uses for auxetic materials, such as knee pads, bulletproof vests, shockproof gloves, explosion-proof drapes, medical dressings, and areas of tissue engineering, for example, artificial blood vessels and artificial folding mucosa [5–7].

Available literature has witnessed the work on helical yarns, woven and composite structures, and warp-knitted and weft-knitted auxetic structures [8, 9]. Knitting technology allows several mesh planar structures and foldable 3D structures with auxetic potential, and this study field is expanding day by day. A warp-knitted fabric is developed using principles of the helical yarn structures with inlay yarn and pillar stitches. Wales are knitted from softer, thicker filaments, and the stiffer yarn is used as inlay. On the application of force, it expands in a widthwise direction on the application of longitudinal force and behaves as an auxetic fabric [10]. NPR of warp-knitted hexagonal structure made from spandex and polyester relies on adopting spandex polyester arrangements in wales. The auxetic behavior of such a structure is more evident in a 45-degree wales-wise direction [11]. A spacer structure is made of two parallelograms mutually aligned in a V shape. Results showed that NPR value is affected by yarn types, the direction of stretching, and the angle between two parallelograms. It delivers better results in the diagonal direction than in the warp and weft direction [12].

In weft knitting, auxetic fabrics are formed based on the re-entrant model, rotating triangles, folded structures, and hexagons and can be formed using a computerized flat-knitting machine [13, 14]. The separate rectangle units can be knitted and then connected on certain vertexes. The results show that the auxetic effect mainly depends on knitted structures. Flat-knitting technology could provide a simple but highly effective way of fabricating auxetic fabrics from conventional yarns [15]. Changing the geometry of the weft-knitted fabric folded structure can be achieved, and these closely folded fabrics typically have more excellent negative Poisson's ratio [16]. Weft-knitted auxetic fabrics were made with high-performance yarns (polyamides). NPR of the developed structures was strongly influenced by the material parameter (fiber type), structural parameter (loop length, cover factor, and yarn density), and machine parameters (takedown tension) [13]. An increase in loop length resulted in a significant improvement in NPR due to the availability of longer yarn lengths in the stitches for structural rearrangement [17]. Another study reveals the influence of stitch length and raw material on the auxetic effect. Samples were made with cotton and acrylic yarns at three different stitch length values, making loose, medium, and tight fabrics [18]. Decreasing values of the stitch length, initial angles of foldable auxetic fabrics also decrease and make fabric tighter, which retain their shape and subsequently show a higher auxetic effect. Regarding the effect of different yarns, acrylic shows a higher auxetic effect [19].

Developing smart and novel structures is one of the most focused research areas in the last three decades [12]. A lot of research has been done in to develop such structures by varying the forming element and their combinations [20–22]. The researchers have developed auxetic fibers [9], yarns [23], fabrics [24], and woven and knitted structures [25]. Some of the knitted structures have a specific application for clothing [26, 27], especially kids wear and maternity clothes, where the comfort of fabric and structure is of high importance. None of the literature is available on the comfort properties of auxetic weft-knitted structures, as per the author's knowledge. The current study focuses on the evaluation of the thermo-physiological comfort of three different auxetic weft-knitted structures made by commonly used yarns for the purpose of clothing. The study also evaluates the auxetic behavior of these knitted structures. The thermo-physiological comfort includes air permeability, overall moisture management capacity (OMMC) and thermal resistance. The findings of this study will be helpful for textile technologies and designers to develop auxetic structures with improved comfort properties for kids' wear and maternity clothes.

2. Materials and Methods

The materials used in this research work were polyester, nylon, acrylic, and cotton yarns having a linear density of 16 tex. Polyester and nylon were used in an intermingled filament form, while cotton and acrylic were in the spun form. Foldable different auxetic structures were made having a combination of face and reverse loops by using a Shima Seiki flat-knitting machine (SVR123SP, Japan), with a gauge of 14, and equipped with the Apex 3 design system. The stitch length was constant (0.42 cm) for all structures. Three different auxetic knitted structures (Figures 1–3) were made using polyester, nylon, acrylic, and cotton yarns.

The factors and their levels are described in Table 1. The design of the experiment (DOE) of the current research work was decided after applying full factorial through the Minitab 17 software on the above two input variables, as given in Table 2.

2.1. Stitch Transfer Process. In the development of auxetic fabrics, a transfer stitch technique was used to make a foldable structure. In a flat-knitting machine, a transfer needle is used for this purpose (Figure 4). For the stitch transfer, a delivering needle is raised above the clearing height with the cams in the carriage, and the loop stretches over the transfer spring (Figure 5). Then, the receiving needle is raised by the cam on the other bed, enters the transfer spring of the delivering needle, and penetrates the loop which will be transferred (Figure 6). The delivering needle moves back, leaving the loop on the receiving needles, and in this way, the loop is transferred to the other loop, as shown in Figure 7.

In single jersey knitting, after transforming the straight yarn into a knitted loop, a loop is joined with bending and twisting forces during the knitting of fabric, and the residual inner force in the produced fabric is stored. These forces can cause the edge to get out of the fabric plane and cause deformation and curling [28]. Weft-knitted auxetic structures can be made by front and back knitting on the flat-knitting machine (Figure 8), and due to the curling effect of the single jersey structure, after relaxation, these structures become foldable, front-knitted loops curls at the back and back knitted loops curls at the front side making the structure foldable. Developed structures are available in Figure 9.

2.2. Characterization

2.2.1. Physical Characteristics. Different physical parameters of all auxetic structures were calculated after knitting. Wales per inch and course per inch were checked using pick glass from 5 different places and calculated the average per standard ASTM D8007-15. Stitch length and stitch density are calculated. The areal density of all auxetic structures was measured according to standard ASTM D3776. The coefficient of friction of yarns to solid material has been checked using ASTM D: 3108-2013.

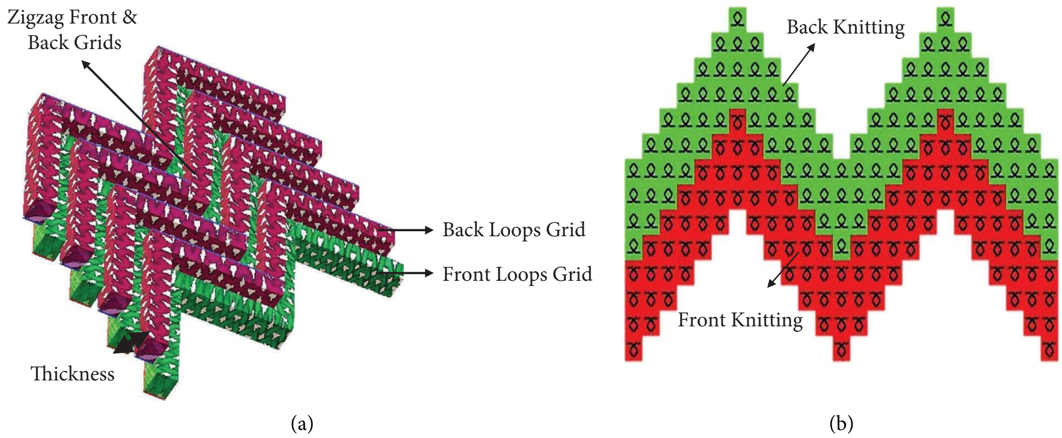

Figure 1: (a) 3D diagram of the zigzag structure and (b) knitting notation of zigzag structures.

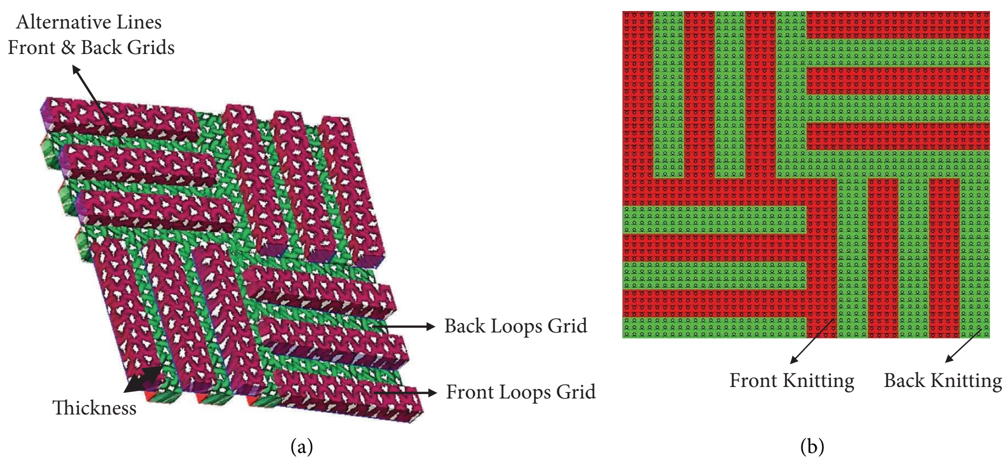

Figure 2: (a) 3D diagram of line structure and (b) knitting notation of line structures.

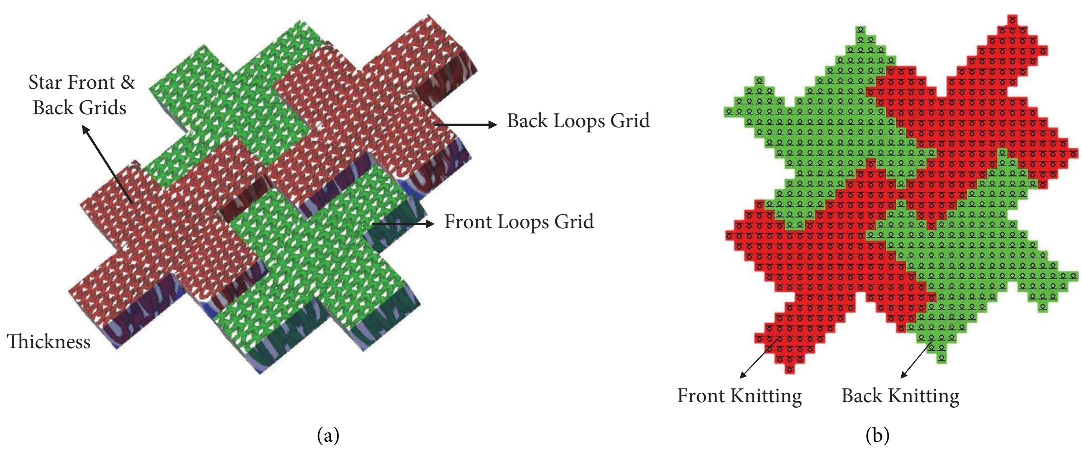

Figure 3: (a) 3D diagram of star structure and (b) knitting notation of star structures.

2.2.2. Negative Poisson's Ratio. A lab-developed standard was followed for the characterization of auxetic behavior. The test was performed on a Universal Testing Machine LLOYD, LRX PLUS. First, samples were placed for 24 hours for conditioning under $65 \pm 2\%$ relative humidity and $20 \pm 2^{\circ}$C temperature. Then, samples are cut to size to fit into the jaws of UTM (100 mm × 150 mm). The effective length of the sample was 100 mm × 100 mm. Samples were clamped,

Table 1: Experimental factors and levels of the research.

Factors	Levels			
	1	2	3	4
Auxetic structures	Zigzag	Star	Lines	
Material	Nylon	Polyester	Acrylic	Cotton

Table 2: Design of experiment of this research.

Structure	Material
Zigzag	Nylon
Zigzag	Polyester
Zigzag	Acrylic
Zigzag	Cotton
Star	Nylon
Star	Polyester
Star	Acrylic
Star	Cotton
Lines	Nylon
Lines	Polyester
Lines	Acrylic
Lines	Cotton

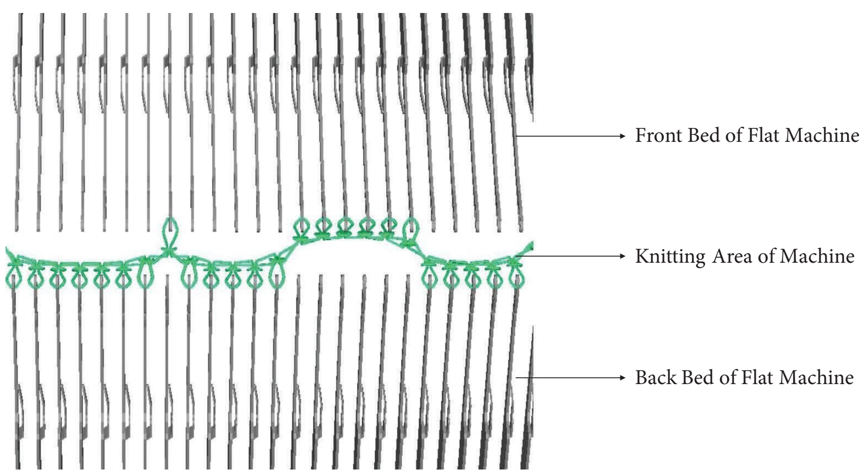

Figure 4: Animated view of auxetic fabric production using apex III.

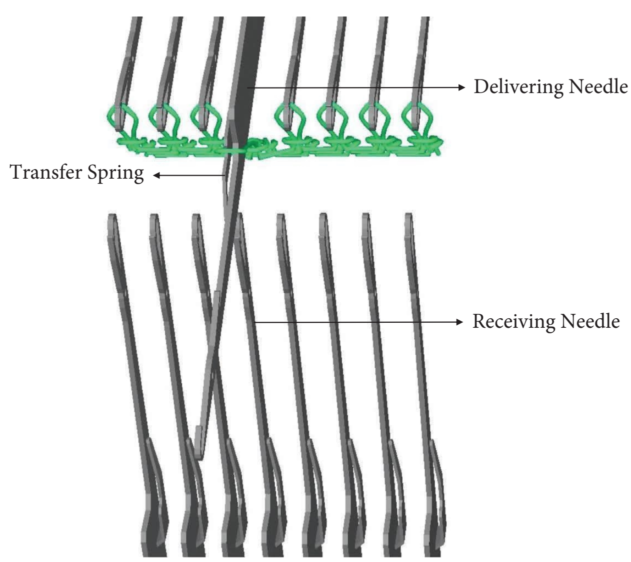

Figure 5: Animated view of delivering needlework during stitch transfer process using the apex III design system.

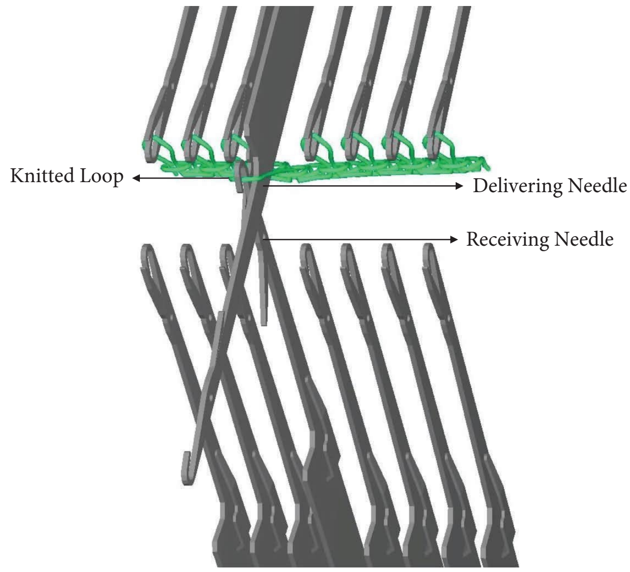

Figure 6: Animated view of receiving needlework during stitch transfer process using the apex III design system.

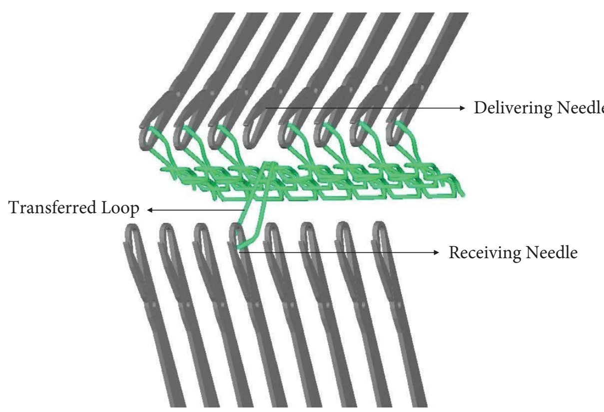

Figure 7: Animated view of transferred stitch using the apex III design system.

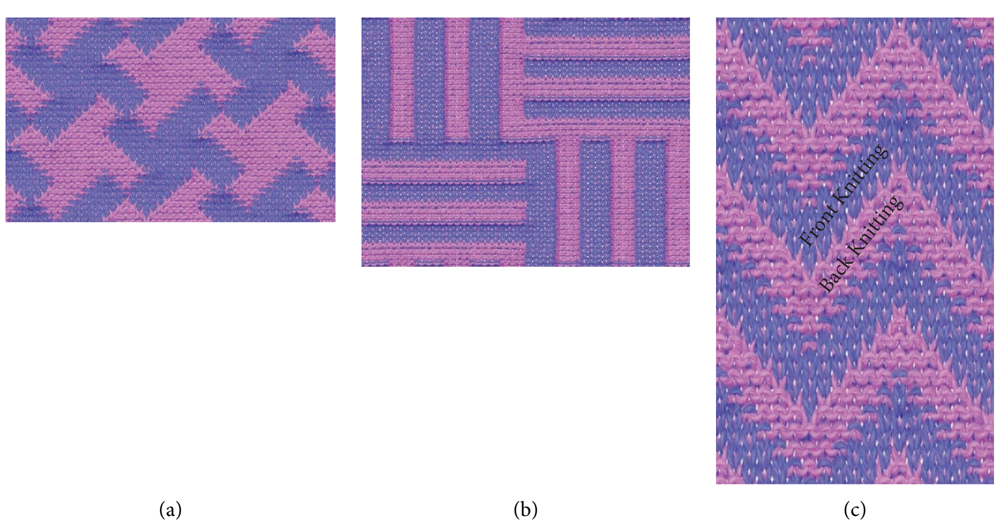

Figure 8: Virtual simulation of structures: (a) star, (b) lines, and (c) zigzag.

FIGURE 9: Developed structures: (a) star, (b) lines, and (c) zigzag.

and a scale was placed behind the specimen to physically take the value of extension or contraction and photographed from the front side by using a camera fixed on a stand. The jaws were moved in a step of 10 mm and then stopped. After each 10 mm movement, a photograph is taken, as shown in Figure 10. This process continues until the extension of 100 mm is reached or the sample shows significant resistance to more stretching. A total of 120 images were taken, 11 images for each sample. The images are then analyzed physically to calculate the extension, and the NPR was calculated using Equations (1)–(3).

The lateral strain (εx), axial strain (εy), and Poisson's ratio (ϑ) were calculated using the following equations:

$$\varepsilon x = \frac{(D_0 - \mathrm{D})}{D_0}, \tag{1}$$

$$\varepsilon y = \frac{(L_0 - \mathrm{L})}{L_o}, \tag{2}$$

$$\vartheta = \frac{-\varepsilon y}{\varepsilon x}. \tag{3}$$

D_0 is the width of the fabric when no force is applied to it, and D is the width of the fabric under force. Thus, L_0 indicates the length of fabric under no force, and L indicates the length of fabric under force.

2.2.3. Thermo-Physiological Comfort. The air permeability of fabric is determined as per ASTM D737-18. This test measures the rate of airflow perpendicular through the fabric under prescribed air pressure. It is an essential feature of the fabric's breathability and is measured in mm/sec. Fabric is placed in the circular test area of 20 cm^2 at an air pressure of 100 Pa. The thermal insulation test is performed according to ISO-11092 standard using the sweating guard hot plate. Specimen of 10/10 inches' dimensions of the fabric placed in the chamber. The temperature and humidity of the air are 20°C and 65% ± 2. The airspeed is specified at 1 m/s at a point 15 mm above the center of the plate surface. The air velocity coefficient of variation due to turbulence is between 5% and 10%. The amount of heat that passes through the specimen is used to calculate the conductivity/insulation value of the specimen and is measured in Km^2/W (Table 3). Liquid moisture management of samples was analyzed on a moisture management tester (SDL-ATLAS, M-290) against standard AATCC 195-2011. Fabric samples are placed between upper and lower concentric moisture sensors to test the ability of the fabric to control liquid moisture. The upper side of the fabric is exposed to a predetermined amount of test solution (synthetic sweat), which subsequently transfers onto the cloth in three directions: (1) extending outward on the fabric's top surface; (2) moving from the top to the bottom of the fabric; (3) moving laterally across the fabric's lower surface before drying up and disappearing. A material's dynamic liquid moisture transport behaviors in these various directions within the material can be evaluated using the measured liquid moisture content. The overall moisture management capacities (OMMC) of all samples were compared. The mean of up to five measurements was calculated [29].

2.2.4. Analysis of Variance (ANOVA). The analysis of variance technique is a statistical method and is employed to recognize the prominent process parameter in the multi-response model. The significance of model phrases is determined in terms of F value or p value. The F value is the ratio of the factor mean square to the mean square error. Usually, a factor with a larger F value has a significant effect on the dependent. The significance of the model parameters can also be identified using p value which is less than α level of significance (5% theoretically). ANOVA is employed to the values of input parameters to identify the significant influence on all the dependent parameters of thermo-physiological comfort for which the p value is less than the level of significance, 5% in this study. The statistical analysis of data was carried out using Minitab 17 software. The p

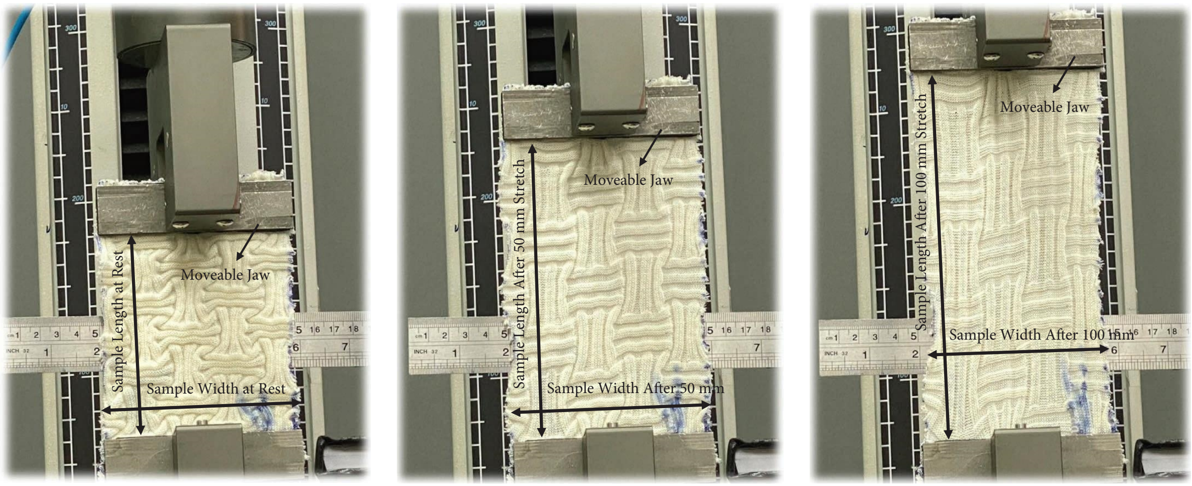

(a) (b) (c)

Figure 10: The behavior of the specimen during the NPR test: (a) sample at rest, (b) sample behavior at 50 mm stretch, and (c) sample behavior at 100 mm stretch.

Table 3: Characterizations with standards and their units.

Sr. no.	Characterization	Standard	Units
1	Physical characterization	ASTM D8007 ASTM D3776	WPI (wales per inch) CPI (courses per inch) g/m^2
2	Coefficient of friction	ASTM D3108	—
3	Negative Poisson's ratio	Lab developed	—
4	Air permeability	ASTM D737	mm/sec
5	Thermal resistance	ASTM D7024	Km^2/W
6	OMMC	AATCC 195	—

Table 4: p values of significant factors for different response variables.

Factors	Air permeability (mm/sec)	Thermal resistance (Km^2/W)	OMMC
Structure	0.198	0.009	0.526
Material	< 0.01	< 0.01	0.217

value (Table 4) shows whether the effect of the input factor on responses is significant or not. It ranges from 0 to 1, and its lower value suggests that the effect of input on output is more significant. Any term with p value >0.05 shows a lack of significance at a confidence level of 95%. Based on the p values in Table 4, the influence of knitted structures is significant in terms of their thermal resistance, but it is insignificant in terms of their air permeability and OMMC value. The material type has a considerable impact on the thermo-physiological properties of smart structures. The p value demonstrates that the effect of material's effect is significant in AP and thermal resistance; however, material type has no impact on the OMMC value. The choice of material is a key consideration for thermo-physiological properties. From Table 4, the type of materials is more important than the fabric's structure. Material's p values are <0.05 for air permeability and thermal resistance, making this factor significant. However, material's p value for moisture handling is 0.217, which is > 0.05, making this factor insignificant. For thermal properties of knitted fabric, structure plays an important role, and its p value of 0.009 makes it a significant factor, whereas the p values for air permeability and OMMC are 0.198 and 0.525, respectively, making them insignificant.

3. Results and Discussion

3.1. Physical Characteristics. The yarn's mechanical properties have been given in Table 5 and the different physical parameters of all specimens were measured after knitting. The detail of the physical parameters of knitted fabrics is given in Table 6.

Stitch length and yarn count are constant in all samples. There is a difference in the WPI and CPI of all samples. All samples are made by the front and reverse knitting on the flat-knitting machine. After front knitting, a stitch is transferred to the back bed for a joint and vice versa. When the fabric relaxes, these folded auxetic structures are formed

Table 5: Mechanical properties of the yarn.

Material type	Count (tex)	Tensile strength (Pa)	Elongation (%)	Twist per inch (TPI)
Nylon	16	6	25.3	0
Polyester	16	5.79	19.25	2
Acrylic	16	3.83	23.18	12.5
Cotton	16	3.39	4.23	18

Table 6: Physical parameters of samples.

Specimen code	Wales per inch	Courses per inch	Stitch length (cm)	Stitch density	GSM (g/m^2)
Nylon zigzag	18	32	0.38	576	399
Polyester zigzag	20	41	0.38	820	566
Acrylic zigzag	21	41	0.38	861	704
Cotton zigzag	19	34	0.38	646	410
Nylon lines	19	35	0.38	665	480
Polyester lines	22	39	0.38	858	633
Acrylic lines	20	37	0.38	740	704
Cotton lines	24	38	0.38	912	530
Nylon star	17	34	0.38	578	380
Polyester star	24	42	0.38	1008	732
Acrylic star	24	38	0.38	912	639
Cotton star	20	36	0.38	720	420

because of structural disequilibrium. The difference in the WPI and CPI is due to the design's geometry change. Star structure shrinks more than lines and zigzag structure, increasing the WPI and CPI of the fabric [30], as given in Table 6. GSM is the weigh-in gram per meter of fabric. The more the fabric shrinks, the more WPI and CPI, causing an increase in the GSM of the folded structure. Star structure shrinks more than lines and zigzag structure and has more GSM than the other two structures [31]. The thickness of the samples is given in Figure 11. Results of friction of materials have been given in Figure 12, and it is clear from the results that polyester has the highest coefficient of friction and nylon has the least.

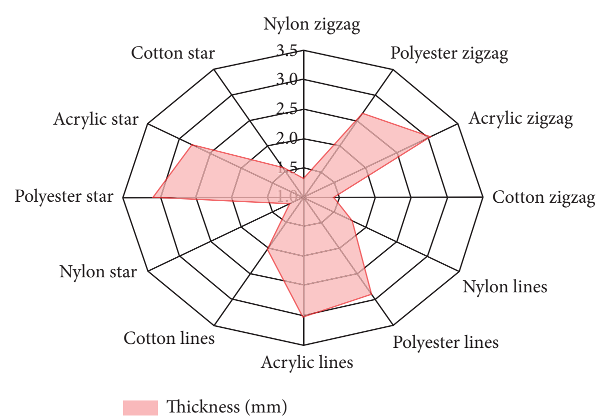

Figure 11: Thickness (mm) of auxetic specimens.

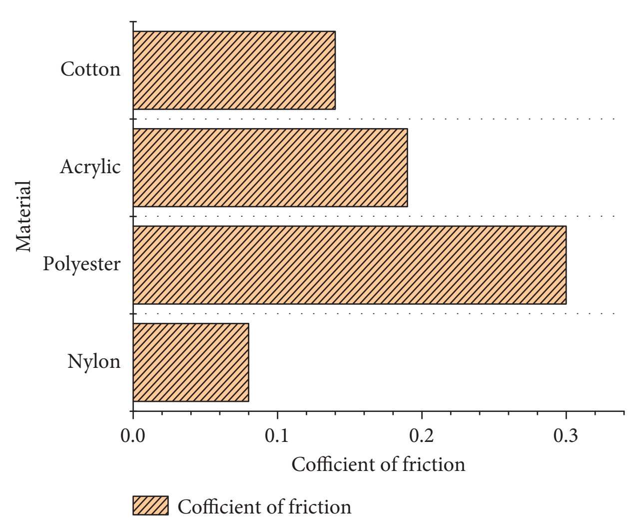

Figure 12: Coefficient of friction of yarns.

3.2. Auxeticity. Figure 13 represents the extension and contraction in the structure when stretching in a course direction in a step of 10 mm. Folded weft-knitted structures can be produced by a combination of front and back loops. Due to the structural disequilibrium and interaction of face and back loops, the fabric shrinks and, after relaxation, becomes a folded weft-knitted fabric [3]. When the fabric is stretched in the lateral direction, a gradual widthwise expansion shows the negative Poisson's ratio (NPR) effect on the opening of the folded structures in both course and wale directions. It is found that the structure made from nylon yarn does not have an extension in the course direction. Samples made with nylon yarn do not fold, and when the force is applied, no extension has been observed, and the structure behaves like normal fabric. While the structures produced by polyester, cotton, and acrylic show expansion in course direction and Figure 14 shows that due to the fabric's unfolding nature, an increasing auxetic effect is achieved when stretching from 20 to 50 mm in a lateral direction. The fabric opens to its fullest after it starts contracting and

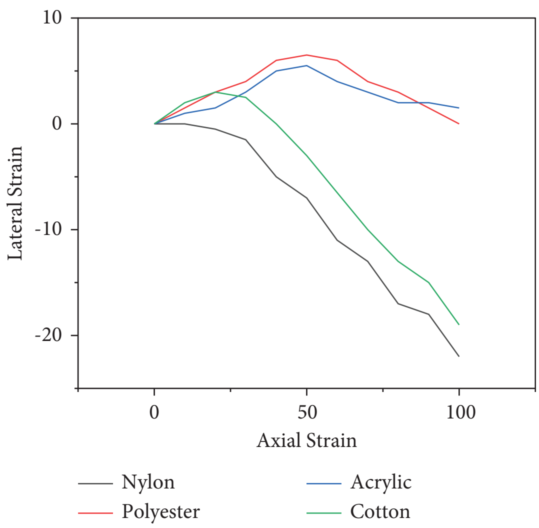

Figure 13: Course-wise expansion in zigzag structure on the application of force.

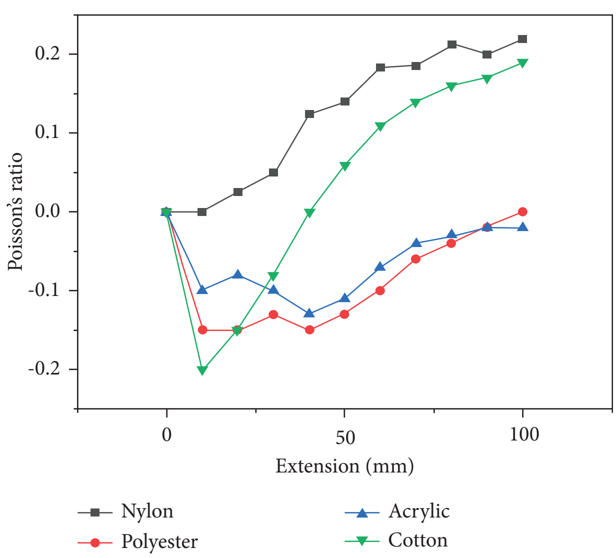

Figure 14: Negative Poisson's ratio of zigzag structures.

behaves like a conventional and nonauxetic structure [23]. Yarn-to-yarn entanglement plays a significant role in the NPR effect [32].

From Figure 14, we can observe that polyester does have the best NPR value due to its rough nature and twist in the yarn. The twisted yarn has less yarn-to-yarn slippage in a knitted structure. When this fabric is stretched in a course direction, it delivers better NPR values, and after a 50 mm extension, it tends to decrease the negative Poisson's effect. Nylon does not show NPR effect due to the zero-twist multifilament in yarn and its soft nature. The coefficient of friction of the yarn surface decreases, which affects the folding of a knitted structure after relaxation [33]. In weft-knitted fabrics, the NPR effect is due to the folding of the fabric [16]. Both acrylic and cotton are spun yarn, but cotton has a lower NPR effect than acrylic due to the soft nature of cotton.

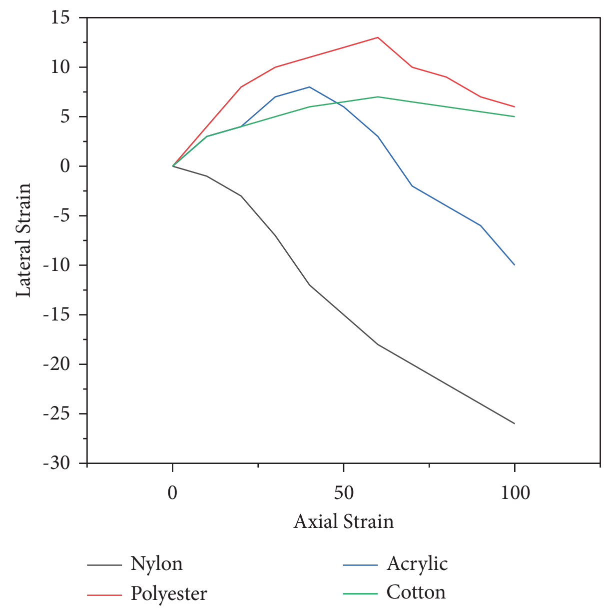

Figure 15: Course-wise expansion in star structure on the application of force.

Figure 15 shows the expansion/contraction in star structure due to the strain applied in course direction, folded Star structure made by the combination of face and back loops, after relaxation due to structural changes in fabric. Folded fabric gains a 3D shape with a thickness mentioned in Figure 11. The same trend of expansion can be seen in this structure. The sample made with nylon showed contraction from the start when the force was applied, and the structure behaves like normal fabric. While the other three structures, polyester, cotton, and acrylic, show extension in course direction.

From Figure 16, we can observe that when the fabric is stretched up to 40 mm an increasing auxetic effect is achieved in cotton, polyester, and acrylic samples, due to the unfolding behavior of the loops in structure. After that fabric starts contracting, the fabric opens to its fullest, and no more expansion is possible, and it begins to behave like a conventional, nonauxetic structure. Polyester offers the best NPR value in star structure. It offers the maximum value at a 10 mm stretch and decreases gradually due to the uneven surface and twist in the yarn. Each structure has different geometry and exhibits accordingly. Yarn with a twist has less yarn-to-yarn slippage in a knitted structure [34]. When the fabric is stretched in a course direction, it exhibits better NPR values. Nylon shows the same NPR effect as star structure due to the zero-twist multifilament of nylon yarn and its soft nature. Cotton shows a less NPR effect than acrylic because of the soft nature of cotton than acrylic and less fiber-to-fiber entanglement with other loop yarn [25].

Figure 17 describes the expansion/reduction in the line structure. Sample made with nylon yarn showed contraction after showing extension at the start i.e., 10 mm when the force was applied, while polyester, cotton, and acrylic structures showed extension up to 50 mm extension in the course direction. Nylon shows the minor auxetic effect only

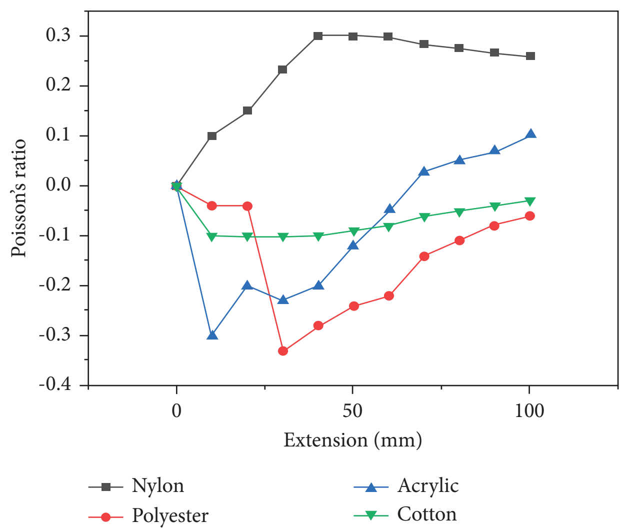

FIGURE 16: Negative Poisson's ratio of star structures.

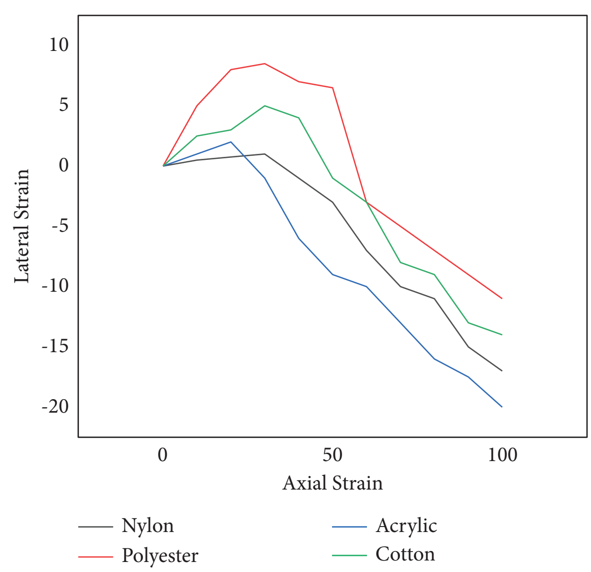

FIGURE 17: Course-wise expansion in line structures on the application of force.

in star structure and can be seen in Figure 18, polyester does the best NPR value at 20 mm stretch and then decreases gradually. Nylon structure shows a minor NPR effect at the start and then its behavior is like conventional fabrics. Cotton shows less NPR effect than acrylic.

Figure 19 describes the structure-wise comparison and the maximum value of NPR of a specific yarn. The arrangement of stitches is the main factor in making a structure auxetic. Polyester offers the maximum value of NPR −0.4 in line structure at 20 mm extension. In lines, structure lines of the front and back stitches are aligned at 90° to each other [35]. On application of force, the folding of the structure opens. At the start, the fabric is fully relaxed, and yarn-to-yarn surface friction is more when a force applied loops open without yarn slippage. As more force is applied, NPR produces a structure, yarn slips from the surface of other yarn, causing a reduction in NPR, and gradually fabric behaves like conventional material. In the polyester case, the unsmooth surface and twist in the yarn take more energy at the start to open the folding, causing a better NPR value than others. Using the appropriate structure and knit pattern makes it possible to produce knitted fabrics with an NPR on a flat-knitting machine [36].

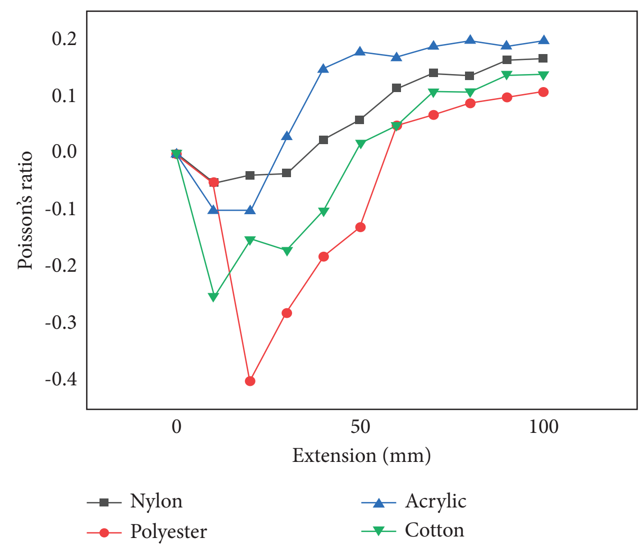

FIGURE 18: Negative Poisson's ratio of line structures.

3.3. Air Permeability. The air permeability of fabric is a very sensitive display in deriving the comfort properties of any textile material. Air permeability can influence the comfort behaviors of the fabric in several ways. The higher air permeability rates are normally attributed to the quickest heat loss obtained from textile materials [37]. If we compare the samples structure-wise (Figure 20), the zigzag structure shows the maximum air permeability than the lines and star structure, because of its structural nature, the zigzag structure shrinks less making the structure less compact and causing increased air permeability of the fabric. The air permeability of the nylon zigzag structure is 540 mm/sec while the other structures' star and lines have less value of AP 510 mm/sec and 530 mm/sec, respectively. In the case of materials, samples made with nylon yarn show promising results of air permeability than acrylic, cotton, and polyester, respectively. From Figure 12, the value of COF of nylon yarn is less than the other materials. Due to this property, structures made with nylon shrinks less and make the structure less compact. Structures made with polyester and acrylic show the least value of AP, i.e., 320 and 290, respectively. If we see the main effect plot of air permeability, a similar trend can be seen in Figure 21.

3.4. Thermal Resistance. Thermal resistance, which is defined as a material's capacity to encapsulate heat rather than convey it, is the most significant factor in determining the thermal comfort of any garment. Air is less heat conductive than any textile fiber, hence the number of dead air pockets has a significant impact on the overall thermal resistance of

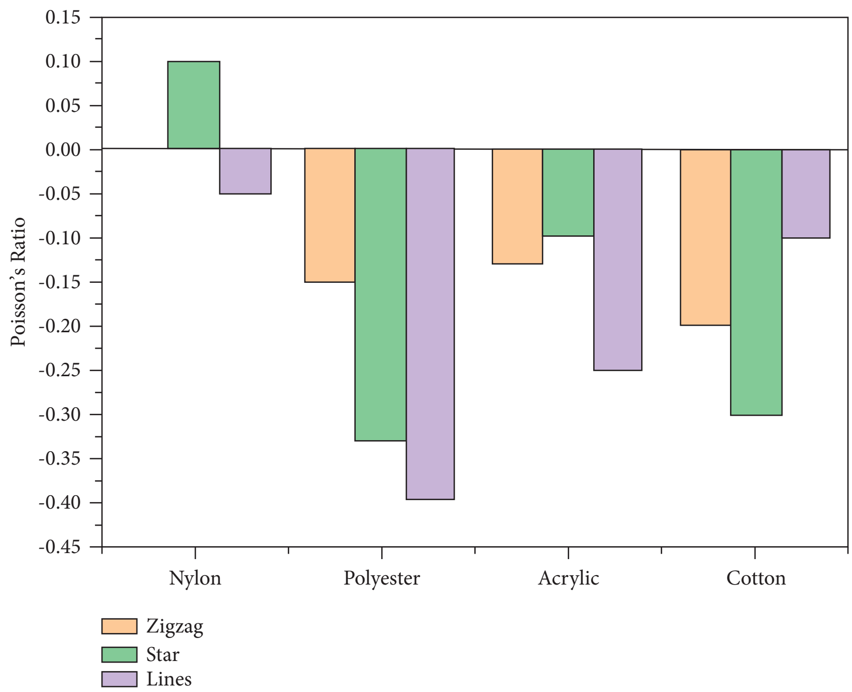

Figure 19: Comparison of NPR of different structures.

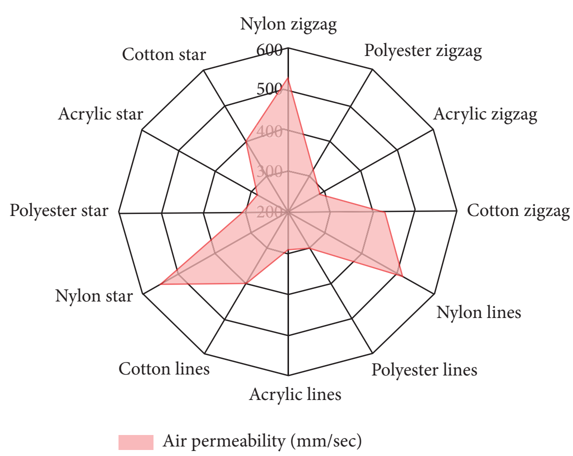

Figure 20: Air permeability of auxetic fabrics.

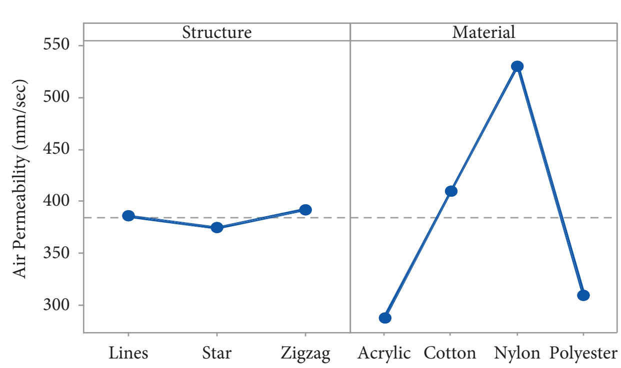

Figure 21: Main effect plot of air permeability.

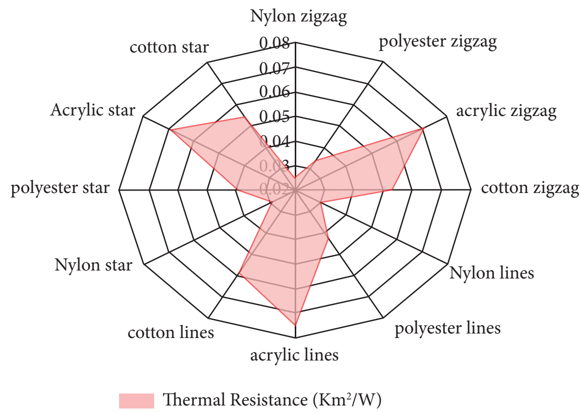

Figure 22: thermal resistance of auxetic fabrics.

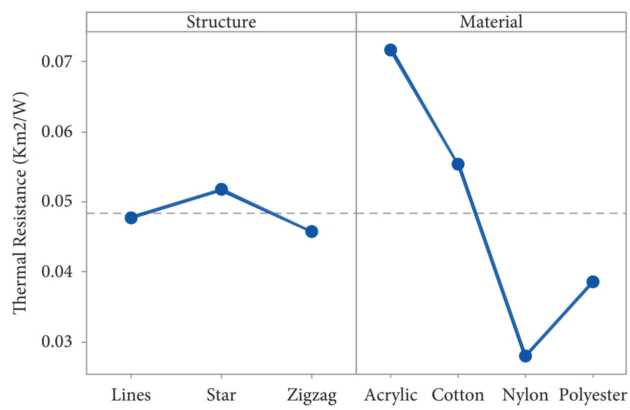

Figure 23: Main effect plot of thermal resistance.

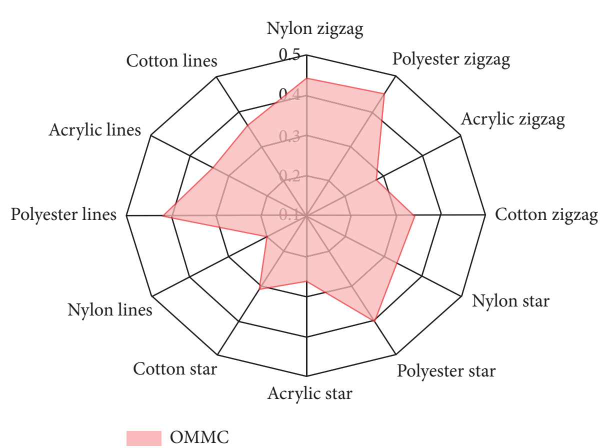

Figure 24: OMMC of auxetic structures.

the fabric. For textile materials, the most essential component for conductivity value is still air in the fabric structure, since still air has the lowest thermal conductivity value of all fibers ($\lambda_{air} = 0.025\ \mathrm{W{\cdot}mK^{-1}}$) [38]. If we compare the samples structure-wise (Figure 22), compared to lines and zigzag structures, the star structure shows the highest thermal resistance 0.75 $\mathrm{Km^2/W}$. This is because, as seen in Figure 8, the more the structure shrinks, the thicker it becomes, creating tight air pockets and so enhancing its heat resistance. In the case of materials, structures made with acrylic yarn have more thermal resistance than cotton, polyester, and nylon. Wet-processed acrylic fibers are extremely porous, including numerous 0.1–1 m microvoids which allows the acrylic fibers to develop wool-like bulkiness [39]. If we

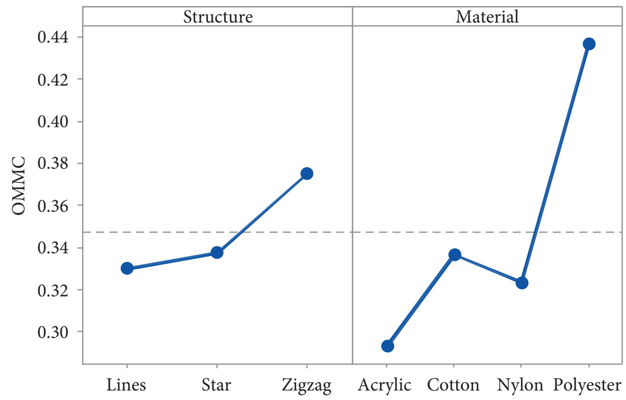

Figure 25: Main effect plot of OMMC.

see the main effect plot of thermal resistance, a similar trend can be seen in Figure 23.

3.5. Overall Moisture Management Capacity (OMMC). Moisture plays an important role in the cooling mechanism of humans. Transferring moisture from the surface of the skin to the atmosphere is an important property for next-to-skin use. OMMC shows the overall management performance of liquid moisture of fabric, and the higher this value, the better the liquid transport performance of fabric [40]. The one-way transport capability property denotes the ability of the fabric to transfer liquid moisture from one side of the fabric to the other side. In other words, a higher one-way transport capability means that sweat can be easily and quickly transferred from the skin to the outer [41]. If we compare the samples structure-wise (Figure 24), the zigzag structure shows the maximum OMMC value than the lines and star structure. Structures made with polyester yarn manage moisture better than the other materials due to the smooth surface of polyester. If we see the main effect plot of OMMC, a similar trend can be seen in Figure 25.

4. Conclusion

Different auxetic weft-knitted fabrics have been developed on Shima Seiki's computerized flat-knitting machines using four types of yarns polyester, nylon, acrylic, and cotton. This research concludes that NPR in weft-knitted auxetic textiles is affected by loop arrangement, material type, yarn surface friction, yarn-to-yarn surface slippage, and knitted structure geometry. By using a flat-knitting machine, these structures can be made due to the possibility of stitch transfer from one needle bed to another. The results also reveal that the NPR exists in all fabrics made from polyester, acrylic, and cotton yarn, but structures made with nylon yarn behave like a conventional knitted fabric.

Thermo-physiological properties show that nylon in zigzag structures provides the best AP value to other specimens. The thermal resistance of acrylic is best in star structures than all other samples and polyester gives the best results of OMMC in zigzag structures. Flat-knitting technology, due to the possibility of stitch transfer from one needle bed to another, can provide a simple but highly effective way of fabricating these fabrics by using conventional yarns as a new structure with nonconventional properties. NPR weft-knitted fabrics will find multiple potential applications in different fields, such as protective wear, medical textile, and sportswear. Further research is needed to explore this area for the potential application of these fabrics.

Data Availability

The data will be made available on request.

Conflicts of Interest

The authors declare that there are no conflicts of interest with respect to the research, authorship, and/or publication of this article.

Acknowledgments

The research was conducted under project GCF-63, funded by Higher Education Commission of Pakistan.

References

[1] Z. Ge and H. Hu, "Innovative three-dimensional fabric structure with negative Poisson's ratio for composite reinforcement," *Textile Research Journal*, vol. 83, no. 5, pp. 543–550, 2013.
[2] H. Kimizuka, H. Kaburaki, and Y. Kogure, "Mechanism for negative Poisson ratios over the α-βTransition of cristobalite, SiO2: a molecular-dynamics study," *Physical Review Letters*, vol. 84, no. 24, pp. 5548–5551, 2000.
[3] H. Hu, M. Zhang, and Y. Liu, "Auxetic textiles," *1st Edition, Woodhead Publishing, Sawston, UK*, pp. 1–358, 2019.
[4] Z. Wang, H. hu, and X. Xiao, "Deformation behaviors of three-dimensional auxetic spacer fabrics," *Textile Research Journal*, vol. 84, no. 13, pp. 1361–1372, 2014.
[5] F. Steffens, S. Rana, and R. Fangueiro, "Development of novel auxetic textile structures using high performance fibres," *Materials & Design*, vol. 106, pp. 81–89, 2016.
[6] K. Luan, A. West, E. Denhartog, and M. Mccord, "Auxetic deformation of the weft-knitted Miura-ori fold," *Textile Research Journal*, vol. 90, no. 5-6, pp. 617–630, 2019.
[7] Y. Sun, W. Xu, W. Wei, P. Ma, and F. Xia, "Stab-resistance of auxetic weft-knitted fabric with Kevlar fibers at quasi-static

loading," *Journal of Industrial Textiles*, vol. 50, no. 9, pp. 1384–1396, 2021.

[8] A. F. W. Coulson, M. E. Baird, and K. W. Mieszkis, "Frictional properties of nylon yarn and their relation to the function of textile guides," *Journal of the Textile Institute Proceedings*, vol. 46, no. 1, pp. P101–P111, 1955.

[9] Z. Ge and H. Hu, "A theoretical analysis of deformation behavior of an innovative 3D auxetic textile structure," *Journal of the Textile Institute*, vol. 106, no. 1, pp. 101–109, 2015.

[10] Y. Liu, H. Hu, J. K. C. Lam, and S. Liu, "Negative Poisson's ratio weft-knitted fabrics," *Textile Research Journal*, vol. 80, no. 9, pp. 856–863, 2010.

[11] S. C. Ugbolue, Y. K. Kim, S. B. Warner et al., "The formation and performance of auxetic textiles. Part II: geometry and structural properties," *Journal of the Textile Institute*, vol. 102, no. 5, pp. 424–433, 2011.

[12] Z. Wang and H. hu, "Auxetic materials and their potential applications in textiles," *Textile Research Journal*, vol. 84, no. 15, pp. 1600–1611, 2014.

[13] M. Glazzard and P. Breedon, "Weft-knitted auxetic textile design," *Physica Status Solidi (B)*, vol. 251, no. 2, pp. 267–272, 2014.

[14] T. Ullah, S. Ahmad, and Y. Nawab, "Development of helical auxetic yarn with negative Poisson's ratio by combinations of different materials and wrapping angle," *Journal of Industrial Textiles*, vol. 51, no. 2, pp. 2181S–2196S, 2020.

[15] K. Alderson, A. Alderson, S. Anand, V. Simkins, S. Nazare, and N. Ravirala, "Auxetic warp knit textile structures," *Physica Status Solidi (B)*, vol. 249, no. 7, pp. 1322–1329, 2012.

[16] W. Xu, Y. Sun, K. R. Raji, and P. Ma, "Design and fabrication of novel auxetic weft-knitted fabrics with Kevlar yarns," *Journal of the Textile Institute*, vol. 110, no. 9, pp. 1257–1262, 2019.

[17] H. Hu, Z. Wang, and S. Liu, "Development of auxetic fabrics using flat knitting technology," *Textile Research Journal*, vol. 81, no. 14, pp. 1493–1502, 2011.

[18] M. Imran Khan, M. Umair, and Y. Nawab, *Use of Auxetic Material for Impact/ballistic Applications*, pp. 199–228, Woodhead Publishing, Sawston, UK, 2021.

[19] S. C. Ugbolue, Y. K. Kim, S. B. Warner et al., "The formation and performance of auxetic textiles. Part I: theoretical and technical considerations," *Journal of the Textile Institute*, vol. 101, no. 7, pp. 660–667, 2010.

[20] A. Ali Shah, M. Shahid, N. A. Siddiqui, and Y. Nawab, "Development of auxetic braided yarns and study the effects of braid angle and material modulus on the negative Poisson's ratio," *Materials Science Forum*, vol. 1068, pp. 101–110, 2022.

[21] H. Iftekhar, R. M. W. Ullah Khan, Y. Nawab, S. T. A. Hamdani, and S. Panchal, "Numerical analysis of binding yarn float length for 3D auxetic structures," *Physica Status Solidi (B)*, vol. 257, no. 10, Article ID 2000440, 2020.

[22] M. U. Nazir, K. Shaker, Y. Nawab, and R. Hussain, "Performance of novel auxetic woven fabrics produced using Helical Auxetic Yarn," *Materials Research Express*, vol. 6, no. 8, Article ID 085703, 2019.

[23] Z. Wang and H. Hu, "Tensile and forming properties of auxetic warp-knitted spacer fabrics," *Textile Research Journal*, vol. 87, no. 16, pp. 1925–1937, 2017.

[24] B. D. Caddock and K. E. Evans, "Microporous materials with negative Poisson's ratios. I. Microstructure and mechanical properties," *Journal of Physics D Applied Physics*, vol. 22, no. 12, pp. 1877–1882, 1989.

[25] Z. Wang and H. Hu, "3D auxetic warp-knitted spacer fabrics," *Physica Status Solidi (B)*, vol. 251, no. 2, pp. 281–288, 2014.

[26] S. Liu and B. Guo, "The impact of the development of modern biotechnology and nanotechnology on the swimming sports industry," *Advances in Materials Science and Engineering*, vol. 2022, Article ID 3303654, 14 pages, 2022.

[27] A. Rasheed, M. H. Malik, F. Ahmad, F. Azam, and S. Ahmad, "Effect of fibers and weave designs on the thermo-physiological comfort of summer scarf fabric," *Advances in Materials Science and Engineering*, vol. 2022, Article ID 8384193, 8 pages, 2022.

[28] W. Ashraf, Y. Nawab, M. Maqsood et al., "Development of seersucker knitted fabric for better comfort properties and aesthetic appearance," *Fibers and Polymers*, vol. 16, no. 3, pp. 699–701, 2015.

[29] M. S. Anas, Z. Azam, M. Waqas, and Z. Gull, "Investigate the effect of inlaid yarn on the mechanical properties and dimension stability of the weft-knitted double Jersey structures for protective application," *Journal of Engineered Fibers and Fabrics*, vol. 17, Article ID 155892502210961, 2022.

[30] S. Ertugrul and N. Ucar, "Predicting bursting strength of cotton plain knitted fabrics using intelligent techniques," *Textile Research Journal*, vol. 70, no. 10, pp. 845–851, 2000.

[31] T. Hassan, M. Q. Khan, A. Salam et al., "The assessment of finishing properties on the mass per unit area, pilling, bursting strength, and wicking behavior of polyester weft-knitted Jersey fabric," *Coatings*, vol. 10, no. 8, 2020.

[32] K. Elizabeth, P. H. Dennis, and C. Fabrics, *A Guide to Improve Shrinkage Performance of Cotton Fabrics*, 2004.

[33] Z. Değirmenci and E. Çoruh, "The influences of loop length and raw material on bursting strength air permeability and physical characteristics of single Jersey knitted fabrics," *Journal of Engineered Fibers and Fabrics*, vol. 12, no. 1, pp. 155892501701200–155892501701249, 2017.

[34] S. Akter, A. Al Faruque, and M. Islam, "Effect of stitch length on different properties of plain single Jersey fabric," *International Journal of Modern Engineering Research*, vol. 7, pp. 71–75, 2017.

[35] K. E. Evans, M. A. Nkansah, and I. J. Hutchinson, "Auxetic foams: modelling negative Poisson's ratios," *Acta Metallurgica et Materialia*, vol. 42, no. 4, pp. 1289–1294, 1994.

[36] J. N. Grima and K. E. Evans, "Auxetic behavior from rotating squares," *Journal of Materials Science Letters*, vol. 19, no. 17, pp. 1563–1565, 2000.

[37] N. Özdil, "A study on thermal comfort properties of the socks," *EÜniversitesi Tekstil Ve Konfeksiyo Dergisi*, vol. 18, pp. 154–158, 2008.

[38] T. Mansoor, L. Hes, Z. Skenderi, H. F. Siddique, S. Hussain, and A. Javed, "Effect of preheat setting process on heat, mass and air transfer in plain socks," *Journal of the Textile Institute*, vol. 110, no. 2, pp. 159–170, 2019.

[39] R. Čiukas, J. Abramavičiute, and P. Kerpauskas, "Investigation of the thermal properties of socks knitted from yarns with peculiar properties, part II: thermal resistance of socks knitted from natural and stretch yarns," *Fibres and Textiles in Eastern Europe*, vol. 86, pp. 64–68, 2011.

[40] H. Avcı, M. Özdemir, B. Y. İridağ, C. S. Duru, and C. Candan, "Comfort properties of socks from seacell fibers," *Journal of the Textile Institute*, vol. 109, no. 3, pp. 419–425, 2018.

[41] M. Hashan, K. M. F. Hasan, and F. R. Khandaker, "Functional properties improvement of socks items using different types of yarn," *International Journal of Textile Science*, vol. 6, pp. 34–42, 2017.